ACCOUNTS of chemical research

pubs.acs.org/accounts Article

Aerosol Acidity: Novel Measurements and Implications for Atmospheric Chemistry

Published as part of the Accounts of Chemical Research special issue "New Frontiers in Chemistry—Climate Interactions".

Andrew P. Ault*

Cite This: https://dx.doi.org/10.1021/acs.accounts.0c00303 Read Online

CONSPECTUS: The pH of a solution is one of its most fundamental chemical properties, impacting reaction pathways and kinetics across every area of chemistry. The atmosphere is no different, with the pH of the condensed phase driving key chemical reactions that ultimately impact global climate in numerous ways. The condensed phase in the atmosphere is comprised of suspended liquid or solid particles, known as the atmospheric aerosol, which are differentiated from cloud droplets by their much smaller size (primarily <10 μm). The pH of the atmospheric aerosol can enhance certain chemical reactions leading to the formation of additional condensed phase mass from lower volatility species (secondary aerosol), alter the optical and water uptake properties of particles, and solubilize metals that can act as key nutrients in nutrient-limited ecosystems or cause oxidative stress after inhalation. However, despite the importance of aerosol acidity for climate and health, our fundamental understanding of pH has been limited due to aerosol size (by number >99% of particles are <1 μm) and complexity. Within a single atmospheric particle, there can be hundreds to thousands of distinct chemical species, varying water content, high ionic strengths, and different phases (liquid, semisolid, and solid). Making aerosol analysis even more challenging, atmospheric particles are constantly evolving through heterogeneous reactions with gases and multiphase chemistry within the condensed phase. Based on these challenges, traditional pH measurements are not feasible, and, for years, indirect and proxy methods were the most common way to estimate aerosol pH, with mixed results. However, aerosol pH needs to be incorporated into climate models to accurately determine which chemical reactions are dominant in the atmosphere. Consequently, experimental measurements that probe pH in atmospherically relevant particles are sorely needed to advance our understanding of aerosol acidity.

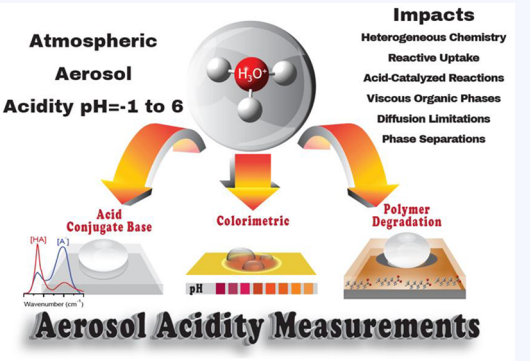

This Account describes recent advances in measurements of aerosol particle acidity, specifically three distinct methods we developed for experimentally determining particle pH. Our acid—conjugate base method uses Raman microspectroscopy to probe an acid (e.g., HSO_4^-) and its conjugate base (e.g., SO_4^{2-}) in individual micrometer-sized particles. Our second approach is a field-deployable colorimetric method based on pH indicators (e.g., thymol blue) and cell phone imaging to provide a simple, low-cost approach to ensemble average (or bulk) pH for particles in distinct size ranges down to a few hundred nanometers in diameter. In our third method, we monitor acid-catalyzed polymer degradation of a thin film (~23 nm) of poly(ε-caprolactone) (PCL) on silicon by individual particles with atomic force microscopy (AFM) after inertially impacting particles of different pH. These measurements are improving our understanding of aerosol pH from a fundamental physical chemistry perspective and have led to initial atmospheric measurements. The impact of aerosol pH on key atmospheric processes, such as secondary organic aerosol (SOA) formation, is discussed. Some unique findings, such as an unexpected size dependence to aerosol pH and kinetic limitations, illustrate that particles are not always in thermodynamic equilibrium with the surrounding gas. The implications of our limited, but improving, understanding of the fundamental chemical concept of pH in the atmospheric aerosol are critical for connecting chemistry and climate.

KEY REFERENCES

- Craig, R. L.; Nandy, L.; Axson, J. L.; Dutcher, C. S.; Ault, A. P. Spectroscopic Determination of Aerosol pH from Acid—Base Equilibria in Inorganic, Organic, and Mixed Systems. *J. Phys. Chem. A* (Veronica Vaida Festschrift),

Received: May 19, 2020

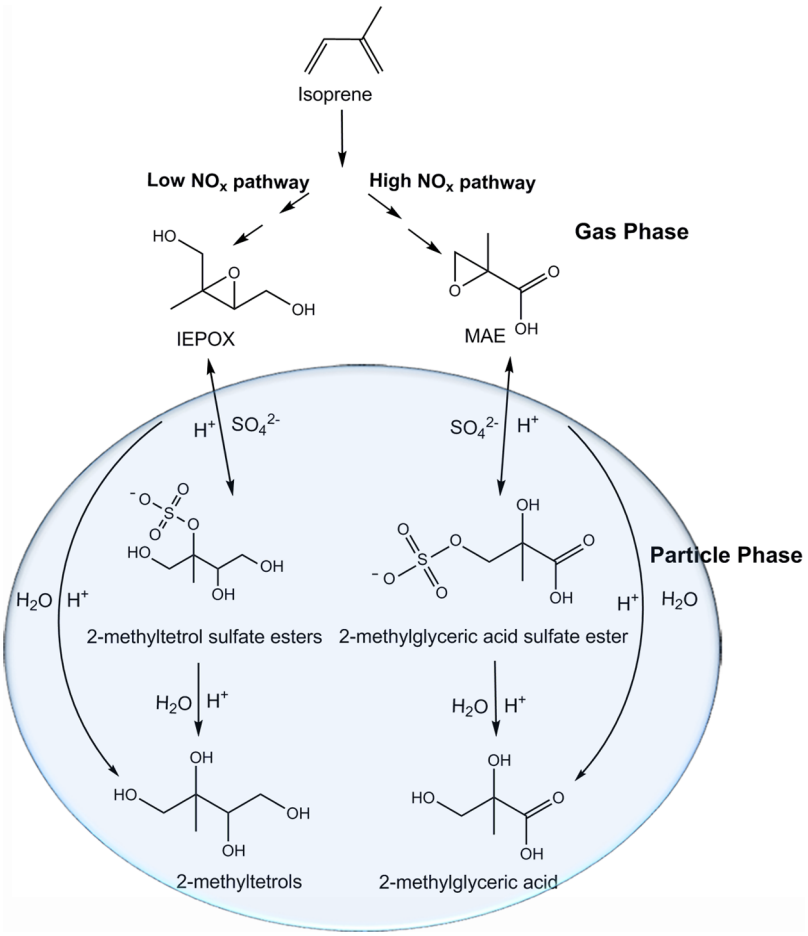

Figure 1. Scheme leading to the formation of isoprene-derived SOA compounds under acidic conditions. Both the high- and low-NO_x pathways are shown forming isoprene epoxydiols (IEPOX) and methacrylic epoxides (MAE). For simplicity, only one isomer of each respective compound is shown. Adapted with permission from ref 2. Copyright 2018 American Chemical Society.

2017, *121*(30), 5690−5699. *Raman microspectroscopy was used to determine single particle pH of micron-sized particles through changes in the acid and conjugate base of a species and was shown for a range of systems (organic, inorganic, and mixed), pH values, and ionic strengths.*[1]

- Bondy, A. L.; Craig, R. L.; Zhang, Z.; Gold, A.; Surratt, J. D.; Ault, A. P. Isoprene-derived organosulfates: Vibrational Mode Analysis by Raman Spectroscopy, Acidity-Dependent Spectral Modes, and Observation in Individual Atmospheric Particles. *J. Phys. Chem. A* **2018**, *122*(1), 303−315. *Vibrational modes in organosulfates were characterized with Raman and density functional theory to identify organosulfates in an ambient sample. The potential for using the protonation state of species intrinsic to secondary organic aerosol (SOA) was also shown.*[2]
- Craig, R. L.; Peterson, P. K.; Nandy, L.; Lei, Z.; Hossain, M. A.; Camarena, S.; Dodson, R. A.; Cook, R. D.; Dutcher, C. S.; Ault, A. P. Direct Determination of Aerosol pH: Size-Resolved Measurements of Submicron and Supermicron Aqueous Particles. *Anal. Chem.* **2018**, *90*(19), 11232−11239. *A low-cost colorimetric method was developed using simple cell-phone camera images to determine the pH of aqueous particles impacted onto pH paper with an impactor. A size dependence to aerosol acidity was observed with a lower pH in smaller particles.*[3]
- Lei, Z.; Bliesner, S. E.; Mattson, C. N.; Cooke, M. E.; Olson, N. E.; Chibwe, K.; Albert, J. N. L.; Ault, A. P. Aerosol Acidity Sensing via Polymer Degradation. *Anal. Chem.* **2020**, *92*(9), 6502−6511. *Polymer degradation was used to determine the acidity of individual ultrafine (<100 nm) particles. Acidic particles were impacted onto poly(ε-caprolactone) (PCL), and the degradation was monitored with atomic force microscopy (AFM), which showed pH-dependent and size-dependent degradation.*[4]

1. INTRODUCTION

1.1. Intro of Aerosol Acidity

The atmospheric aerosol, a collection of liquid or solid particles suspended in the atmosphere, impacts climate by scattering and absorbing solar radiation, as well as nucleating cloud droplets and ice crystals.[5,6] When considering Earth's radiative balance, the direct (scattering and absorption) and indirect (nucleating and modifying cloud properties) effects of the atmospheric aerosol represent the most uncertain aspects of climate change.[5,6] An important contribution to atmospheric aerosol driven climate uncertainty is that each particle is an incredibly complex chemical environment,[7] and the properties of water within these suspended particles are critically important for their impacts on climate.[8,9] Aerosol particles range in size from molecular clusters of a few nanometers to tens of micrometers with >10^{13} molecules and properties resembling bulk materials, with the most important size range for direct and indirect aerosol effects being roughly 50 to 1,000 nm in diameter, commonly

https://dx.doi.org/10.1021/acs.accounts.0c00303
Acc. Chem. Res. XXXX, XXX, XXX−XXX

referred to as the accumulation mode.[10] In addition to their wide size range, aerosol particles are continuously changing as they undergo reactions with trace gases (heterogeneous reactions) and aqueous and organic phase reactions in the condensed phase.[11] Though complex, the pH of an aerosol particle is still a critical property that determines which heterogeneous and condensed reactions occur, as well as their kinetics, as is true in most subdisciplines of chemistry.

The sources of particles in the atmosphere are either primary, where particles are directly emitted as solids or liquids, or secondary, where species emitted as gases undergo reactions that either 1) lower their vapor pressure to the point they condense on existing particles or 2) undergo heterogeneous uptake reactions where they rapidly react to form a lower volatility species after colliding with a particle.[10] Secondary aerosol is a large fraction of aerosol mass below 1 μm both from inorganic species (SO_4^{2-}, NO_3^-, and NH_4^+) and organic species (secondary organic aerosol, SOA).[12] To illustrate the importance of aerosol pH, it is useful to discuss one of the most abundant types of aerosol and how pH-dependent reactions affects it. Isoprene is a key precursor gas to SOA formation and has the highest emissions of any nonmethane hydrocarbon to the atmosphere.[13] Isoprene is a very reactive five carbon molecule with two double bonds (Figure 1) and forms lower volatility species after atmospheric oxidation reactions with the hydroxyl (OH) radical.[2] Paulot et al. found that epoxides are important oxidation products of isoprene,[14] with examples including isoprene epoxydiols (IEPOX) and methacrylic acid epoxides (MAE) (Figure 1),[15−17] which can lead to a large fraction of SOA.[18] These epoxides then undergo acid-catalyzed ring opening reactions after heterogeneous uptake,[19] which lead to substantially higher SOA formation with initially acidic particles versus more neutral particles.[20] This is reflected in the much shorter lifetimes of IEPOX in particles with pH = 1 (minutes) versus pH = 4 (days).[21] In addition to being a key factor in SOA formation, pH also impacts the formation of secondary inorganic aerosol, by determining the dominant reaction pathways for haze events in Beijing and other urban megacities.[22−24] pH also determines the impacts of particles after deposition, as dissolution of minerals and metals impacts their ability to act as nutrients (e.g., iron or phosphate),[25,26] or health impacts after inhalation by solubilizing toxic transition metals (e.g., copper).[27] Thus, pH plays a key role in determining how much secondary aerosol forms, as well as the impacts of particles after removal from the atmosphere.

Determining the pH of an atmospheric particle or collection of particles is incredibly challenging, as unlike beaker-scale experiments, you cannot place a standard electrochemical pH probe in a particle with a diameter <1 μm. pH is determined by the activity of the H^+ ion (a_{H^+}) (eq 1)

$$\mathrm{pH} = -\log_{10}(a_{H^+}) = -\log_{10}(\gamma_{H^+}[H^+]) \quad (1)$$

where γ_{H^+} is the activity coefficient of the H^+ ion, and $[H^+]$ is the molar concentration of H^+ (more formally IUPAC uses a molality-based version of pH).[28] Given that activity coefficients depend on ionic strength, it is also important not to change the amount of water present in particles when measuring a particle's pH.[28] This is inconsistent with how most atmospheric particles are collected for chemical analysis, as they typically involve either pulling air through a filter (where collected particles rapidly dry), heating particles, or pulling the particles into vacuum, which can dry or even freeze them.[29] Thus, our understanding of aerosol acidity to date has primarily been guided by proxy or indirect methods.[30] These proxy methods were reviewed by Hennigan et al.,[31] who pointed out a number of weaknesses and flaws that make them unreliable. For example, the ion balance method (eq 2) assumes that all charged species other than chloride, nitrate, sulfate, and ammonium are H^+ ions.

$$[H^+] = \sum n_i[anion_i] - \sum n_i[cation_i] = [Cl^-] + [NO_3^-] + 2[SO_4^{2-}] - [NH_4^+] \quad (2)$$

This is problematic as accumulation mode particles are often half organic by mass,[12,32] with many deprotonated and, thus, charged species (e.g., dicarboxylic acids, amines, organosulfates, etc.). These particles can also contain hundreds to thousands of organic species in a single particle,[12,32] which makes this type of balancing method challenging. Given the limitation of proxy methods, many researchers have turned to the phase-partitioning method, which monitors a semivolatile species with an appreciable fraction in both the gas (e.g., $NH_{3(g)}$) and particle phases (e.g., $NH_{4(aq)}^+$). While phase partitioning has provided the most reliable measurements to date, it relies on expensive instruments to measuring gases like ammonia (NH_3) and nitric acid (HNO_3) that are challenging to sample, as well as an underlying assumption that the system is at thermodynamic equilibrium between gas and particle phases. However, there have been indications that kinetic limitations to diffusion and partitioning may be important,[33−37] highlighting the need for acidity measurements that determine pH solely based on species in the condensed phase. Due to measurement limitations, models such as E-AIM,[38,39] ISORROPIA,[40] AIOMFAC,[41,42] and MOSAIC[43] have been utilized to explore aerosol pH and account for much of our current understanding.

Pye et al.[44] recently reviewed the state of acidity in aerosols and clouds based on our current knowledge from measurements and models. There were 467 measurements of cloudwater pH, but only 47 measurements of aerosol pH globally, primarily from phase partitioning. However, despite the limited number of measurements, the understanding of pH that emerged was that atmospheric aerosols are typically highly acidic (pH = −0.5 to 5, median pH = 2.5). For fine particulate matter (particles < 2.5 μm), a pH < 2 was most common and lower than for coarse particles > 2.5 μm.[44] The oxidation of SO_2 provides an example of why low pH values are observed. SO_2 can undergo gas phase oxidation to H_2SO_4, which then partitions to particles due to a very low vapor pressure, or it forms in the particle (i.e., condensed) phase via oxidation due to H_2O_2.[45] pH values < 2 are consistent with prior model predictions showing sustained highly acidic particles in the southeast U.S. (pH ∼ 1), even with decreasing SO_2 emissions.[46] However, in regions with higher emission of NH_3 (e.g., Beijing) models predict pH can be closer to neutral (pH ∼ 5).[23] However, as noted in Pye et al.,[44] direct measurements of aerosol pH are needed to fill in our gaps in understanding how pH changes spatially, diurnally, and across particle sizes.

Particle-to-particle variability of chemical composition further complicates pH measurements,[47] and particle-to-particle variability in pH is poorly understood.[4] If each particle is thought of as a tiny atmospheric beaker with no walls, a particle from the ocean will be very different than from a car or from a forest fire.[48] Pye et al. showed that particles from different sources likely have different pH values,[44] but there have been minimal measurements exploring this for ambient particles. This means that even if the average pH for all particles in a given size

https://dx.doi.org/10.1021/acs.accounts.0c00303
Acc. Chem. Res. XXXX, XXX, XXX−XXX

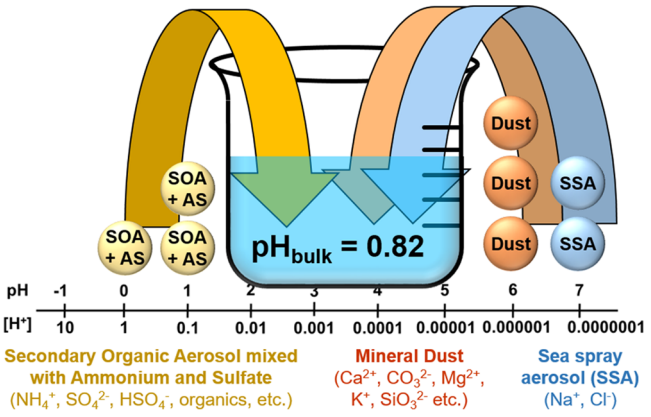

Figure 2. Example of why reporting an average pH can be suboptimal. Three acidic particles (SOA, ammonium, sulfate, and bisulfate) with pH = 0, 1, and 1 dominate the bulk pH even with three mineral dust particles of pH = 6 and two sea spray aerosol particles of pH = 7. Despite fewer very acidic particles, the bulk pH is highly acidic.

range is known, the particle-to-particle variability in pH will not necessarily be known.[49] Given that pH is on a logarithmic scale (eq 1), this makes the need for individual particle measurements of pH even more important. Figure 2 shows an example of how an average or "bulk" pH provides an incomplete picture of aerosol acidity and, thus, the impacts of aerosol pH on key reactions. In addition, the pH of an individual particle evolves over its atmospheric lifetime, such as when an initially pH 7−8 sea spray aerosol (SSA) reacts with HNO_3 or H_2SO_4 and pH decreases.[50−52] Thus, measurements are needed to address the multiple knowledge gaps regarding aerosol acidity: 1) direct measurements of pH in atmospheric particles, 2) measurements of size-resolved aerosol acidity, and 3) measurements of individual particle pH to explore particle-to-particle variability in pH.

Overcoming the current lack of measurements for atmospheric aerosol pH has been a focus of my research group for the past 5 years, which we have approached from a number of different experimental perspectives. We developed a spectroscopic acid−conjugate base method using vibrational spectroscopy of individual particles,[1,53] a colorimetric method using pH-sensitive indicators to measure size-resolved bulk pH,[3] and a method measuring polymer degradation from individual particles with atomic force microscopy (AFM).[4] The development of the different methods, the scientific insights that have been gained regarding aerosol acidity, and the bigger picture implications of aerosol acidity are explored below.

2. TECHNIQUES USED

2.1. Generation and Collection of Aerosol

Aerosol particles were generated with either a Collison nebulizer (a.k.a. atomizer) for large samples or a Meinhard nebulizer for small samples. Bulk solution pH was monitored with a standard pH probe (Mettler Toledo FE20). Aerosol was collected with inertial impactors, which use well-defined flow through precisely machined holes of a set diameter to separate particles based on their aerodynamic diameter (d_a) and collect them onto specifically chosen filters or substrates. Ambient aerosol and some lab samples were collected using a three-stage micro-analysis particle sampler (MPS, California Measurements, Inc., 2 lpm) with 50% aerodynamic cut-points giving aerodynamic diameter ranges of 2.8−5.0 μm, 0.4−2.8 μm, and <0.4 μm, respectively. An eight-stage mini-MOUDI (Model 135, MSP Corp., 2 lpm) was used for some studies, with aerodynamic cut-points of 320−560 nm, 180−320 nm, and <180 nm, for the stages used.

2.2. Raman Microspectroscopy

Raman microspectroscopy provides a useful tool for probing individual aerosol particles spectroscopically under ambient relative humidity (RH) and temperature conditions. Our work primarily used a LabRAM HR Evolution Raman micro-spectrometer from Horiba with a 532 nm laser (50 mW) and 0.6 or 1.8 cm^{-1} resolution (1800 or 600 gr/mm gratings). Work below has primarily utilized a 100×, 0.9 N.A. objective and 100×, 0.6 N.A. long working distance objective, which analyzes particles within an RH and temperature-controlled microscope stage (Linkham LTS120). Particles analyzed by Raman were typically impacted on small, quartz microscope slides placed in the MPS or mini-MOUDI. Further details are available in our prior publications.[1,4,54−57]

2.3. Atomic Force Microscopy (AFM)

AFM is very sensitive to changes in height, phase, and morphology of particles, with detection capable at thicknesses down to a nanometer, which is far less than the thickness of an aerosol impacted on a surface. As with Raman, AFM is operated at ambient RH, temperature, and pressure. The AFM imaging used below was primarily conducted on a PicoPlus 5500 AFM (Agilent) with NanoScience tips with a resonance frequency of 300 kHz and a force constant of 40 N/m. All AFM discussed herein was of particles impacted on silicon or polymer-coated silicon wafers.

2.4. Atomic Force Microscopy with Photothermal Infrared (AFM-PTIR) Spectroscopy

One of the traditional limitations of AFM has been a lack of chemical information. While infrared (IR) spectroscopy can provide detailed and quantitative functional group information, IR microscopy has traditionally been limited to large particles (>10 μm in diameter) due to the diffraction limit of IR light.[7] This size limitation has made the application of IR to individual particle studies challenging as >99% of atmospheric particles in the atmosphere at any given time are <1 μm in diameter. Recently, AFM coupled with photothermal infrared spectroscopy (AFM-PTIR) has emerged as a method capable of simultaneously probing physical and chemical properties of nanoscale features.[58] The fundamental principle is that as an OPO or QCL laser is scanned across the mid-IR, the particle expands as a vibrational mode of the material in the sample absorbs at a specific frequency. This photothermal effect is detected by the AFM tip, and a spectrum is obtained by processing the change in deflection. Our group was the first to apply AFM-PTIR to atmospheric aerosols in Bondy et al.[59] We have continued to use AFM-PTIR,[4,60] as have several other research groups,[61,62] to study a range of environmental questions ranging from Arctic aerosol composition to indoor surface chemistry to pH. In Olson et al.,[63] we recently were the first to probe aerosol particles with optical PTIR (O-PTIR) with simultaneous Raman microspectroscopy. This method builds on our AFM-PTIR work[59] but detects photothermal changes in scattering of a 532 nm laser,[63] instead of deflection of an AFM tip.

https://dx.doi.org/10.1021/acs.accounts.0c00303
Acc. Chem. Res. XXXX, XXX, XXX−XXX

3. RESULTS AND DISCUSSION

3.1. New Measurements of Aerosol Acidity

3.1.1. Acid−Conjugate Base Method. Acids and their conjugate bases provide important information about the pH of a system, particularly near the pK_a for a specific [HA] and [A^-] pair. We initially sought to determine the pH of an individual particle using species that would be common in the atmospheric aerosol.[53] While a single 100 nm atmospheric particle can contain hundreds to thousands of organic species, there is a far more limited set of inorganic ions in most atmospheric particles. Among the most abundant are sulfate, nitrate, ammonium, and chloride,[10] of which the former three are all molecular ions that can be probed with vibrational spectroscopy. A key advantage of vibrational spectroscopy is that the frequency of the vibrational modes associated with the protonated acid and deprotonated conjugate base is often separated by at least 50 cm^{-1}. We focused first on sulfate as it is both very abundant and nonvolatile, making it an ideal model ion to use in laboratory studies. Since the sulfate−bisulfate pK_a is 1.99 (eq 3),[64] both sulfate (SO_4^{2-}) and bisulfate (HSO_4^-) should be present in atmospheric aerosol under different pH conditions (reaction 1).

$$HSO_4^-{}_{(aq)} \leftrightarrow H^+{}_{(aq)} + SO_4^{2-}{}_{(aq)} \quad \text{(R1)}$$

In Rindelaub et al.,[53] we used the acid dissociation equation for the sulfate−bisulfate equilibrium to solve for the H^+ concentration with magnesium sulfate particles roughly 5−10 μm in diameter. Figure 3 shows the relative fraction of bisulfate and sulfate, as well as the increasing ionic strength at low pH.

$$K_a = \frac{\gamma_{H^+}[H^+]\gamma_{SO_4^{2-}}[SO_4^{2-}]}{\gamma_{HSO_4^-}[HSO_4^-]} = 0.0102 \quad (3)$$

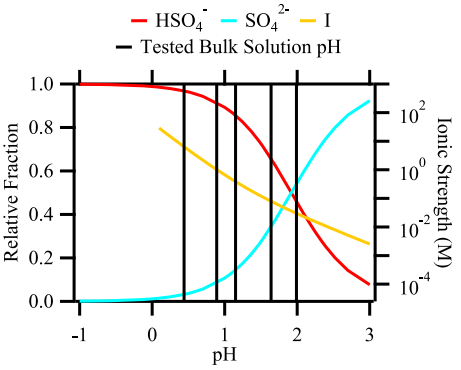

Figure 3. Relative fraction for HSO_4^- (red) and SO_4^{2-} (blue) concentrations, as well as ionic strength (I) (yellow), as a function of pH using the dissociation constant (K_a = 0.01) assuming equilibrium conditions. Each tested bulk solution pH (0.44, 0.89, 1.15, 1.64, and 1.99) is highlighted in black. Reprinted with permission from ref 53. Copyright 2016 American Chemical Society.

The method consists of two key steps: 1) generating calibration curves for [HSO_4^-] and [SO_4^{2-}] and 2) determining activity coefficients for the three ions in eq 3: [HSO_4^-], [SO_4^{2-}], and [H^+]. Ionic strength is a complicating factor, as it can be quite high at low pH, leading to activity coefficients far from unity. Activity coefficients were calculated with the extended Debye−Hückel equation, though this begins to have issues above an ionic strength of 0.1 M, which can require more complicated calculations.[53,65] Figure 4 shows the shift from

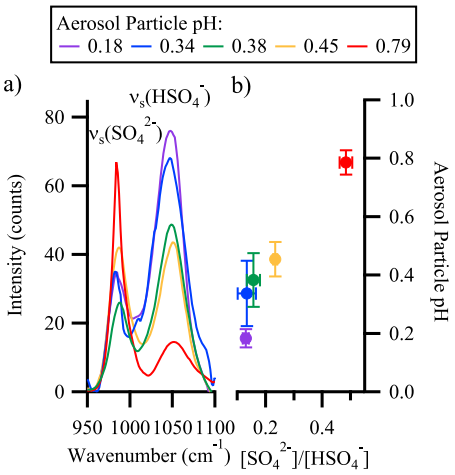

Figure 4. a) Raman spectra of $\nu_s(SO_4^{2-})$ and $\nu_s(HSO_4^-)$ for initial aerosol particles generated from each seed aerosol bulk solution (left) and b) average aerosol pH as a function of $[SO_4^{2-}]/[HSO_4^-]$ (right). Error bars are based on the standard deviation for multiple trials. Reprinted with permission from ref 53. Copyright 2016 American Chemical Society.

sulfate to bisulfate as particle pH becomes more acidic using calibration curves based on peak areas. After demonstrating the validity of the measurement, we explored the change in pH that would occur over a diurnal (daily) RH cycle (35−80%). We found that pH could shift between 0.5 and 1.0 pH units, which is in line with model predictions for the Southeast U.S.[66] We also observed that particle pH was lower than for the bulk solution, which has also been observed in subsequent studies.

After establishing that the acid−conjugate base method could work for individual aerosol particles, the pH range was expanded using a range of inorganic and organic salts commonly observed in atmosphere aerosol in Craig et al.[1] Importantly for atmospheric relevance, the particles in this Account were mostly in the 2−3 μm size range, near the upper diameter of fine particulate matter (PM) at 2.5 μm, which is the EPA regulated size-fraction most strongly connected with negative health effects.[67] Figure 5 shows the different systems the method was expanded to cover, including nitric acid/nitrate (HNO_3/NO_3^-, pK_a = 1.3), bioxalate/oxalate ($HC_2O_4^-/C_2O_4^{2-}$, pK_a = 3.81), acetic acid/acetate (CH_3COOH/CH_3COO^-, pK_a = 4.76), and

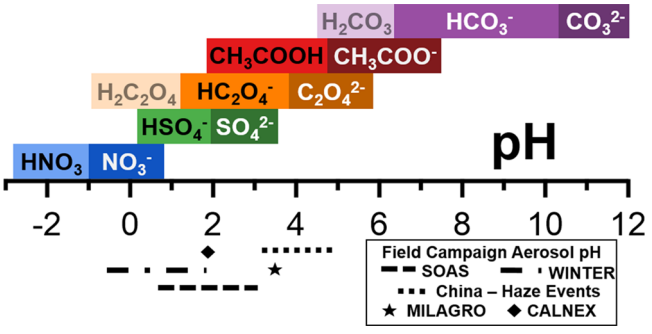

Figure 5. Schematic showing dominant species present as a function of pH for each acid−base system studied, as well as a comparison to the aerosol pH predicted by thermodynamic models for several field campaigns. $H_2C_2O_4$ and H_2CO_3 are included but cannot be quantified with this method. Adapted with permission from ref 1. Copyright 2017 American Chemical Society.

https://dx.doi.org/10.1021/acs.accounts.0c00303
Acc. Chem. Res. XXXX, XXX, XXX−XXX

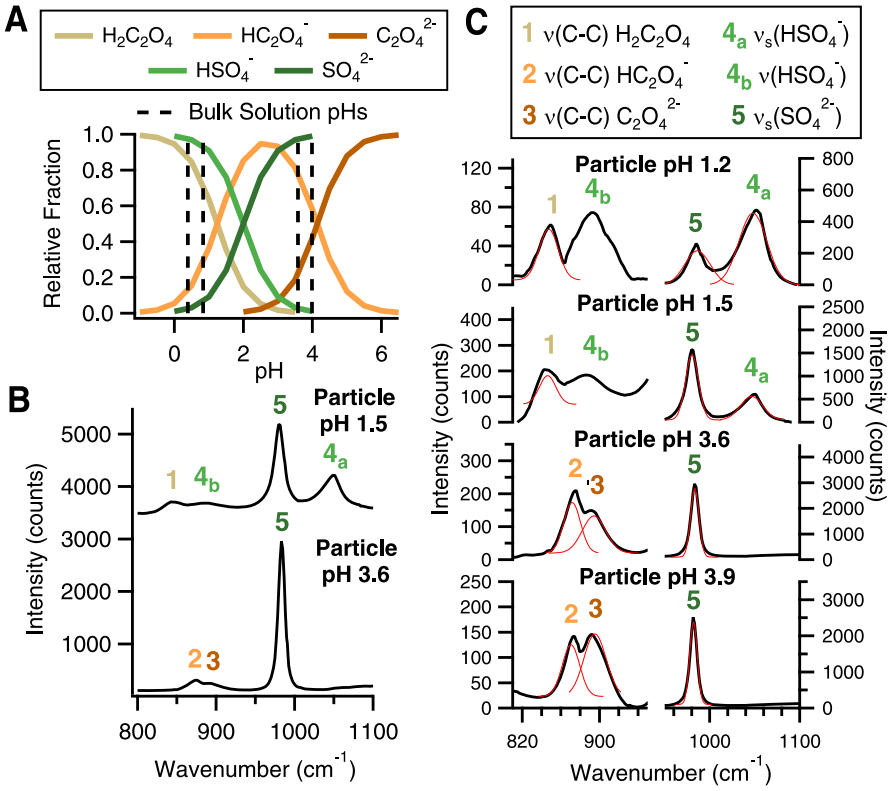

Figure 6. (A) Relative fraction as a function of pH for oxalic acid and bioxalate equilibrium and sulfuric acid equilibrium, with the pH of the bulk solutions used to generate oxalate-sulfate mixed aerosol particles highlighted by the dashed lines. (B) Full Raman spectra for $HC_2O_4^-/C_2O_4^{2-}$ and HSO_4^-/SO_4^{2-} mixed aerosol particles pH 1.5 and 3.2. (C) Raman spectra for $HC_2O_4^-/C_2O_4^{2-}$ and HSO_4^-/SO_4^{2-} aerosol particles pH 1.2, 1.5, 3.6, and 3.9 focused on spectral regions where ν(C−C) $HC_2O_4^-$, ν(C−C) $C_2O_4^{2-}$, $\nu_s(HSO_4^-)$, and $\nu_s(SO_4^{2-})$ are present. Red lines indicate Gaussian peak fits. Reprinted with permission from ref 1. Copyright 2017 American Chemical Society.

bicarbonate/carbonate (HCO_3^-/CO_3^{2-}, pK_a = 10.30).[1,64] To move beyond individual salts to more complicated systems, we also studied a mixture of ammonium sulfate and oxalic acid and were able to use equilibria from both sulfate/bisulfate and oxalic acid/bioxalate/oxalate to determine the pH of individual particles in Figure 6. One of the challenges of calculating pH using the most prevalent thermodynamic models is that they either do not include organic species (a large portion of submicron aerosol mass) or only include a few species. To explore this further, the activity coefficients of the H^+ ion for the inorganic, organic, and mixed system were compared. The inorganic-only system had high ionic strengths (>10 mol/kg, molality-based) leading to an activity coefficient for H^+ as low as 0.68, while the organic systems and mixtures had lower ionic strengths (<4 mol/kg) and activity coefficients for H^+ that only decreased to 0.72. That the organic−inorganic mixture had ionic strengths more similar to the organic than traditionally considered inorganic systems highlights the need to include organic species when trying to determine the pH of an individual aerosol.

An advantage of the acid−conjugate base method is that we do not need to use indicator ions but rather can rely on the vibrational modes of species already present in the aerosol. In Bondy et al.,[2] we used Raman microspectroscopy and density functional theory (DFT) calculations to explore the molecular structure of two important classes of organosulfates formed through acid-catalyzed reactions in the atmosphere (methyltetrol sulfate esters and methylglyceric acid sulfate esters), as well as their hydrolysis products (methyltetrols and methylglyceric acid). These two sets of SOA species form from isoprene oxidation under either low-NO_x (methyltetrols and methyltetrols sulfate esters) or high NO_x (methylglyceric acid and methyl glyceric acid sulfate ester) conditions (Figure 1). The methylglyceric acid molecules have a carboxylic acid group, but the pK_a was not known, though glyceric acid has a pK_a = 3.5.[2] Thus, we were able to monitor the acid−conjugate base transition by increasing the pH above the likely pK_a (Figure 7).

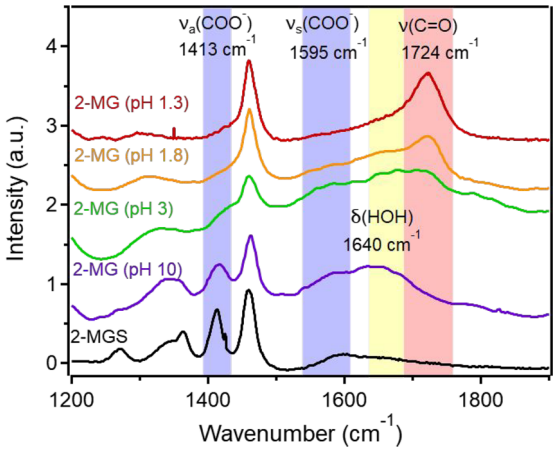

Figure 7. Aqueous phase experimental Raman spectra of 2-methylglyceric acid sulfate ester (2-MGS) and 2-methylglyceric acid (2-MG) at varying pH. Note the decrease in the carbonyl at 1724 cm^{-1} and the increase in carboxylate peaks at 1413 and 1595 with increasing pH. Reprinted with permission from ref 2. Copyright 2018 American Chemical Society.

https://dx.doi.org/10.1021/acs.accounts.0c00303
Acc. Chem. Res. XXXX, XXX, XXX−XXX

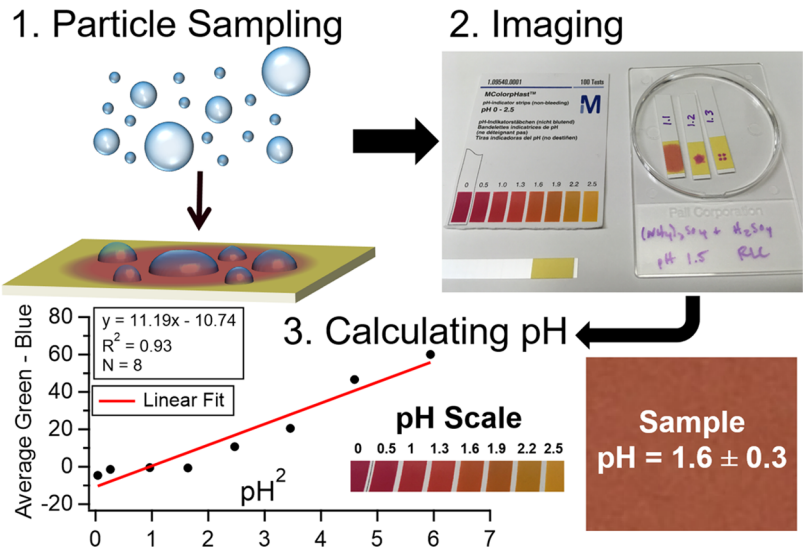

Figure 8. Schematic of the pH indicator paper method for direct measurement of aerosol pH. Adapted with permission from ref 3. Copyright 2018 American Chemical Society.

Below the pK_a the protonated carboxylic acid had a strong carbonyl peak at 1724 cm^{-1}. As the pH was increased by adding sodium hydroxide (NaOH), the carbonyl peak decreased, while the symmetric and asymmetric vibrations associated with the deprotonated carboxylate group were observed at 1413 and 1595 cm^{-1}, respectively.[2] In working with more complicated systems, the ability to leverage the intrinsic protonation state of molecules already present in the aerosol indicates that the acid−conjugate base method has significant potential for future application.

3.1.2. Colorimetric Method. Low cost methods that can be easily deployed in the field are still needed that can probe the pH of particles in the ambient atmosphere, as the acid−conjugate base method above requires collection and transport to an expensive Raman microspectrometer, which is challenging without the sample being altered. Colorimetric indicator pH has been used for decades to monitor pH in numerous applications, but applying the method quantitatively to aerosol had been challenging. In Craig et al.,[3] we developed a method to image colorimetric indicator paper (thymol blue with pK_a = 1.7 and methyl orange with pK_a = 3.47) with a cell phone camera after impaction of aqueous aerosol.

The cell phone image is converted to pH^2 by relating the average green−blue pixel intensity to a calibration curve (Figure 8). For particles < 2.5 μm, the method was quite sensitive and able to detect ∼65 μg of impacted particles. It is important to note that the aerosol must be aqueous for this method to work. This method was applied in the field to generate size-resolved pH measurements at both a rural and an urban site in Michigan.[3] An intriguing observation from this method was that for particles with pH below the pK_a of sulfate−bisulfate (1.99),[64] the smaller particles were significantly more acidic than the larger particles (Figure 9).[3] This was confirmed via the acid−conjugate base method using Raman.[3]

3.1.3. Polymer Degradation Method. Our third aerosol acidity method uses degradation of a pH-sensitive polymer, monitored with AFM, to determine the acidity of individual submicron particles. In Lei et al.,[4] aerosols were generated with known pH, which was verified with the colorimetric method. These particles were deposited onto 23 ± 2 nm poly(ε-caprolactone) (PCL) films on silicon wafers, produced by

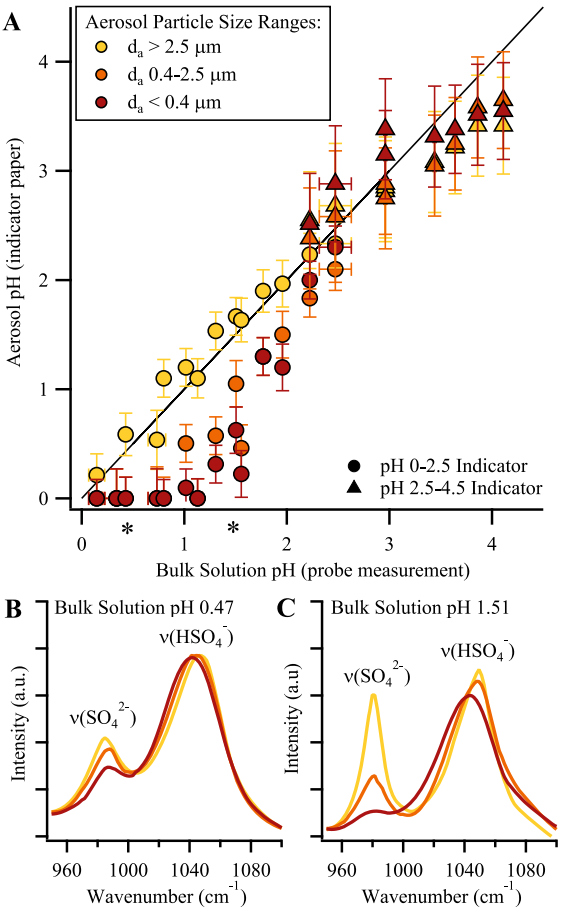

Figure 9. (A) pH indicator paper measurements of aerosol particles d_a > 2.5 μm (yellow), d_a 0.4−2.5 μm (orange), and d_a < 0.4 μm (red) as a function of the bulk solution pH from which the particles were generated. Raman spectra of the $\nu(SO_4^{2-})$ and $\nu(HSO_4^-)$ modes, normalized to the $\nu(HSO_4^-)$ mode, for particles generated from bulk solution (B) pH 0.47 and (C) pH 1.51 (corresponding data marked by the *). Reprinted with permission from ref 3. Copyright 2018 American Chemical Society.

https://dx.doi.org/10.1021/acs.accounts.0c00303
Acc. Chem. Res. XXXX, XXX, XXX−XXX

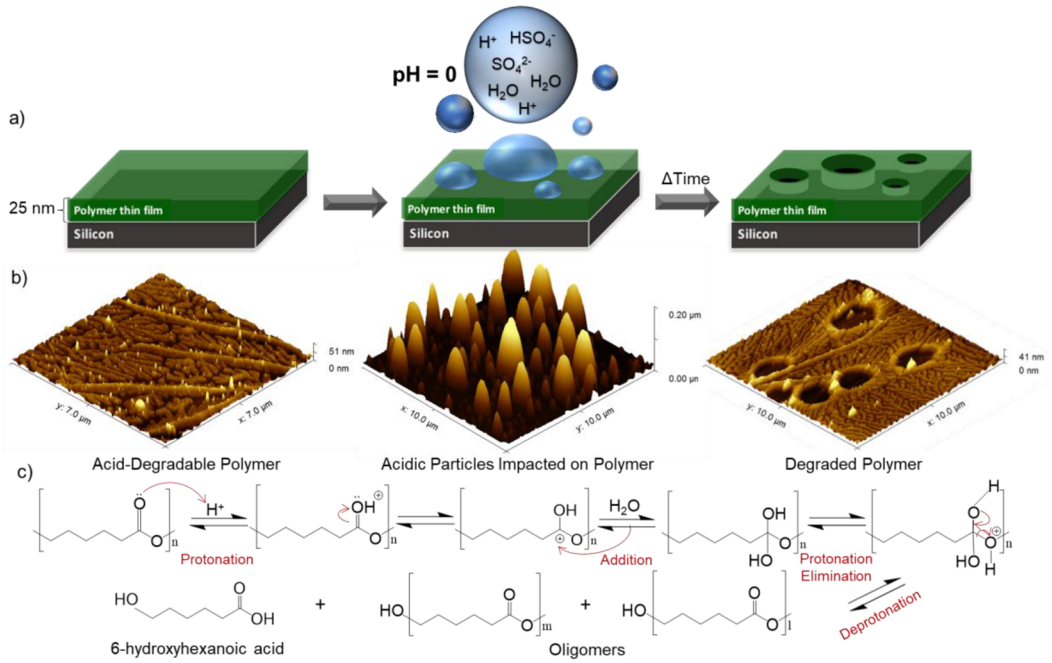

Figure 10. a) Schematic depicting the use of PCL thin film degradation for determining aerosol acidity; b) AFM 3D height image of the PCL degradation process, the size (length × width × height) of AFM images from left to right are 7 μm × 7 μm × 51 nm, 10 μm × 10 μm × 0.2 μm, and 10 μm × 10 μm × 41 nm; and c) acid-catalyzed degradation mechanism of PCL. Note that "*n*" refers to the number of repeat units in the starting PCL material and that l + *m* < *n*. Adapted with permission from ref 4. Copyright 2020 American Chemical Society.

collaborator Prof. Julie Albert at Tulane University. Acidic particles (pH = 0) degraded the PCL (Figure 10). The extent of degradation (holes remaining after washing off the particles) was determined via AFM and related back to the particle pH. In addition, the degradation mechanism was monitored spectroscopically through changes in the PCL carbonyl stretch and the C−H stretching region with Raman spectroscopy. As degradation is directly related to the $[H^+]$, the response was based on individual aerosol properties without the need for gas phase measurements and was able to probe aerosol of different sizes (100−1,000 nm) after inertial impaction on the polymer.

4. SUMMARY

The importance of aerosol acidity on atmospheric chemistry has been discussed, and three different methods developed to experimentally determine pH in particles have been described: 1) acid−conjugate base method, 2) colorimetric method, and 3) polymer degradation method. Each pH method has strengths and limitations requiring a multimethod approach to fully understand aerosol pH. For example, acid−conjugate base and polymer degradation are both single particle, while colorimetric is bulk. Both colorimetric and polymer degradation can probe accumulation mode particles, while acid−conjugate base with Raman cannot. Lastly, both acid−conjugate base and colorimetric can provide rapid pH data, while polymer degradation is slow. Thus, further method development is needed for atmospheric aerosol pH measurements, though other groups are already using these approaches in the laboratory.[68−70] Taken together, our knowledge of aerosol acidity from these novel methods is improving, but considerable work remains.

5. FUTURE RESEARCH DIRECTIONS

Based on the research discussed above, there are a number of different avenues to further our understanding of aerosol acidity impacts on atmospheric chemistry.

- The largest step forward would result from further development of these methods or other methods that enable a reliable ambient measurement of aerosol pH.
- The size dependence of aerosol acidity between fine and coarse mode particles has been predicted by models and shown with the measurements above. However, a more detailed understanding of how aerosol pH changes as a function of size is needed, particularly in the context of atmospheric conditions (e.g., diurnal cycles of RH and emissions).[71] This would also enable improved parametrizations in models.
- The potential for particle-to-particle variability in pH is a highly debated topic, particularly for submicrometer aerosol particles. Direct measurements that can probe this would be useful to understand how broad the pH distribution is for particles at one size and over the full size distribution. Figure 2 above notes the result that a range of pH values across particles could lead to, but most exploration of atmospheric aerosol pH has not been based on direct individual particle measurements.
- The interplay between organic and aqueous phases merits further exploration. As noted by Freedman et al.,[72] liquid liquid phase separations exhibit pH-dependent behavior, but little experimental data is available regarding the activity of the H^+ ion in organic matrices, only model predictions.[73] Two recent Zhang et al. papers showed that the interplay between pH and phase had substantial impacts on predicted SOA formation based on modeling of flow tube results,[36,74] which has subsequently been expanded to regional air quality models to predict SOA reduction due to core−shell morphologies.[75] In addition, the evolution of organic phases due to chemical changes, such as for organosulfates,[76] has recently highlighted our need to understand pH evolution in individual particles.[54] Further understanding as to how the interplay between

https://dx.doi.org/10.1021/acs.accounts.0c00303
Acc. Chem. Res. XXXX, XXX, XXX−XXX

pH and phase further impacts SOA formation for organic phases remains an active area of research.[36]

- Accounting for different phases and their viscosities becomes even more challenging when considering that many particles are a mixture of liquid, semisolid, and solid phases and the aqueous component of any individual particle will be in equilibrium between aqueous and nonaqueous portions of the particle, as well as the gas phase and the aqueous phase (e.g., $NH_{3(g)}$ and $NH_4^+{}_{(aq)}$). Thus, pH in multicomponent and multiphase particles merits further investigation.
- Lastly, considerable physical chemistry work has informed our understanding of water and pH behavior in confined spaces and at interfaces,[77−80] where properties substantially different than those observed in a beaker-scale are found.[81] As small pockets of water in otherwise viscous organic aerosol could exhibit similar behavior, there remain lessons to be learned and new research directions available by exploring confined spaces and interfaces within aerosols and their atmospheric impacts.

AUTHOR INFORMATION

Corresponding Author

Andrew P. Ault − *Department of Chemistry, University of Michigan, Ann Arbor, Michigan 48109, United States;* orcid.org/0000-0002-7313-8559; Phone: 734-763-2283; Email: aulta@umich.edu

Complete contact information is available at: https://pubs.acs.org/10.1021/acs.accounts.0c00303

Notes

The author declares no competing financial interest.

Biography

Andrew Phillip Ault is the Dow Corning Assistant Professor of Chemistry in the Department of Chemistry at the University of Michigan. He obtained his B. A. in Chemistry from Carleton College beginning his work on aerosols with Prof. Deborah Gross. He received his Ph.D. in Chemistry from the University of California, San Diego under the guidance of Prof. Kim Prather. He completed postdoctoral positions at the University of British Columbia with Prof. Ruth Signorell and at the University of Iowa with Prof. Vicki Grassian as part of the Center for Aerosol Impacts of Chemistry of the Environment (CAICE) a Center for Chemical Innovation (CCI) funded by the National Science Foundation (NSF). He started his independent career at the University of Michigan in 2013, and his laboratory focuses on probing atmospheric aerosols through spectroscopic and microscopic methods. He received a NSF CAREER award from the Division of Chemistry and was chosen as an Alfred P. Sloan Research Fellow in Chemistry (2018).

ACKNOWLEDGMENTS

All of the collaborators are gratefully acknowledged, particularly Prof. Jason Surratt (University of North Carolina − Chapel Hill), Prof. Cari Dutcher (University of Minnesota), and Prof. Julie Albert (Tulane University). Funding for the work above was provided by NSF CAREER Grant CHE-1654149, NSF Award AGS-1506768, and the Alfred P. Sloan Foundation Research Fellowship (Chemistry) G-2018-11239. Nicole Olson, Ziying Lei, and Madeline Cooke are thanked for their comments on the manuscript, and Ziying Lei is thanked for assistance with the conspectus figure.

REFERENCES

(1) Craig, R. L.; Nandy, L.; Axson, J. L.; Dutcher, C. S.; Ault, A. P. Spectroscopic Determination of Aerosol pH from Acid−Base Equilibria in Inorganic, Organic, and Mixed Systems. *J. Phys. Chem. A* **2017**, *121*, 5690−5699.

(2) Bondy, A. L.; Craig, R. L.; Zhang, Z.; Gold, A.; Surratt, J. D.; Ault, A. P. Isoprene-Derived Organosulfates: Vibrational Mode Analysis by Raman Spectroscopy, Acidity-Dependent Spectral Modes, and Observation in Individual Atmospheric Particles. *J. Phys. Chem. A* **2018**, *122*, 303−315.

(3) Craig, R. L.; Peterson, P. K.; Nandy, L.; Lei, Z.; Hossain, M. A.; Camarena, S.; Dodson, R. A.; Cook, R. D.; Dutcher, C. S.; Ault, A. P. Direct Determination of Aerosol pH: Size-Resolved Measurements of Submicrometer and Supermicrometer Aqueous Particles. *Anal. Chem.* **2018**, *90*, 11232−11239.

(4) Lei, Z.; Bliesner, S. E.; Mattson, C. N.; Cooke, M. E.; Olson, N. E.; Chibwe, K.; Albert, J. N. L.; Ault, A. P. Aerosol Acidity Sensing via Polymer Degradation. *Anal. Chem.* **2020**, *92*, 6502−6511.

(5) Ravishankara, A. R.; Rudich, Y.; Wuebbles, D. J. Physical Chemistry of Climate Metrics. *Chem. Rev.* **2015**, *115*, 3682−3703.

(6) IPCC *Climate Change 2013: The Physical Science Basis. Contribution of Working Group I to the Fifth Assessment Report of the Intergovernmental Panel on Climate Change*; Stocker, T. F., Qin, D., Plattner, G.-K., Tignor, M., Allen, S. K., Boschung, J., Nauels, A., Xia, Y., Bex, V., Midgley, P. M., Eds.; Cambridge, United Kingdom and New York, NY, USA, 2013; 1535pp.

(7) Ault, A. P.; Axson, J. L. Atmospheric Aerosol Chemistry: Spectroscopic and Microscopic Advances. *Anal. Chem.* **2017**, *89*, 430−452.

(8) Rubasinghege, G.; Grassian, V. H. Role(s) of adsorbed water in the surface chemistry of environmental interfaces. *Chem. Commun.* **2013**, *49*, 3071−3094.

(9) Farmer, D. K.; Cappa, C. D.; Kreidenweis, S. M. Atmospheric Processes and Their Controlling Influence on Cloud Condensation Nuclei Activity. *Chem. Rev.* **2015**, *115*, 4199−4217.

(10) Seinfeld, J. H.; Pandis, S. N. *Atmospheric chemistry and physics: from air pollution to climate change*; John Wiley & Sons: 2016.

(11) Abbatt, J. P. D.; Lee, A. K. Y.; Thornton, J. A. Quantifying trace gas uptake to tropospheric aerosol: recent advances and remaining challenges. *Chem. Soc. Rev.* **2012**, *41*, 6555−6581.

(12) Zhang, Q.; Jimenez, J. L.; Canagaratna, M. R.; Allan, J. D.; Coe, H.; Ulbrich, I.; Alfarra, M. R.; Takami, A.; Middlebrook, A. M.; Sun, Y. L.; Dzepina, K.; Dunlea, E.; Docherty, K.; DeCarlo, P. F.; Salcedo, D.; Onasch, T.; Jayne, J. T.; Miyoshi, T.; Shimono, A.; Hatakeyama, S.; Takegawa, N.; Kondo, Y.; Schneider, J.; Drewnick, F.; Borrmann, S.; Weimer, S.; Demerjian, K.; Williams, P.; Bower, K.; Bahreini, R.; Cottrell, L.; Griffin, R. J.; Rautiainen, J.; Sun, J. Y.; Zhang, Y. M.; Worsnop, D. R. Ubiquity and dominance of oxygenated species in organic aerosols in anthropogenically-influenced Northern Hemisphere midlatitudes. *Geophys. Res. Lett.* **2007**, *34*, L13801.

(13) Guenther, A.; Karl, T.; Harley, P.; Wiedinmyer, C.; Palmer, P. I.; Geron, C. Estimates of global terrestrial isoprene emissions using MEGAN (Model of Emissions of Gases and Aerosols from Nature). *Atmos. Chem. Phys.* **2006**, *6*, 3181−3210.

(14) Paulot, F.; Crounse, J. D.; Kjaergaard, H. G.; Kurten, A., St; Clair, J. M.; Seinfeld, J. H.; Wennberg, P. O. Unexpected Epoxide Formation in the Gas-Phase Photooxidation of Isoprene. *Science* **2009**, *325*, 730−733.

(15) Lin, Y. H.; Knipping, E. M.; Edgerton, E. S.; Shaw, S. L.; Surratt, J. D. Investigating the influences of SO2 and NH3 levels on isoprene-derived secondary organic aerosol formation using conditional sampling approaches. *Atmos. Chem. Phys.* **2013**, *13*, 8457−8470.

(16) Surratt, J. D.; Chan, A. W. H.; Eddingsaas, N. C.; Chan, M.; Loza, C. L.; Kwan, A. J.; Hersey, S. P.; Flagan, R. C.; Wennberg, P. O.; Seinfeld, J. H.; Finlayson-Pitts, B. J. Reactive intermediates revealed in

https://dx.doi.org/10.1021/acs.accounts.0c00303
Acc. Chem. Res. XXXX, XXX, XXX−XXX

secondary organic aerosol formation from isoprene. *Proc. Natl. Acad. Sci. U. S. A.* **2010**, *107*, 6640−6645.
(17) Nguyen, T. B.; Bates, K. H.; Crounse, J. D.; Schwantes, R. H.; Zhang, X.; Kjaergaard, H. G.; Surratt, J. D.; Lin, P.; Laskin, A.; Seinfeld, J. H.; Wennberg, P. O. Mechanism of the hydroxyl radical oxidation of methacryloyl peroxynitrate (MPAN) and its pathway toward secondary organic aerosol formation in the atmosphere. *Phys. Chem. Chem. Phys.* **2015**, *17*, 17914−17926.
(18) Budisulistiorini, S. H.; Baumann, K.; Edgerton, E. S.; Bairai, S. T.; Mueller, S.; Shaw, S. L.; Knipping, E. M.; Gold, A.; Surratt, J. D. Seasonal characterization of submicron aerosol chemical composition and organic aerosol sources in the southeastern United States: Atlanta, Georgia,and Look Rock, Tennessee. *Atmos. Chem. Phys.* **2016**, *16*, 5171−5189.
(19) Surratt, J. D.; Chan, A. W. H.; Eddingsaas, N. C.; Chan, M. N.; Loza, C. L.; Kwan, A. J.; Hersey, S. P.; Flagan, R. C.; Wennberg, P. O.; Seinfeld, J. H. Reactive intermediates revealed in secondary organic aerosol formation from isoprene. *Proc. Natl. Acad. Sci. U. S. A.* **2010**, *107*, 6640−6645.
(20) Lin, Y. H.; Zhang, Z. F.; Docherty, K. S.; Zhang, H. F.; Budisulistiorini, S. H.; Rubitschun, C. L.; Shaw, S. L.; Knipping, E. M.; Edgerton, E. S.; Kleindienst, T. E.; Gold, A.; Surratt, J. D. Isoprene Epoxydiols as Precursors to Secondary Organic Aerosol Formation: Acid-Catalyzed Reactive Uptake Studies with Authentic Compounds. *Environ. Sci. Technol.* **2012**, *46*, 250−258.
(21) Gaston, C. J.; Riedel, T. P.; Zhang, Z. F.; Gold, A.; Surratt, J. D.; Thornton, J. A. Reactive Uptake of an Isoprene-Derived Epoxydiol to Submicron Aerosol Particles. *Environ. Sci. Technol.* **2014**, *48*, 11178−11186.
(22) Wang, G.; Zhang, R.; Gomez, M. E.; Yang, L.; Zamora, M. L.; Hu, M.; Lin, Y.; Peng, J.; Guo, S.; Meng, J.; Li, J.; Cheng, C.; Hu, T.; Ren, Y.; Wang, Y.; Gao, J.; Cao, J.; An, Z.; Zhou, W.; Li, G.; Wang, J.; Tian, P.; Marrero-Ortiz, W.; Secrest, J.; Du, Z.; Zheng, J.; Shang, D.; Zeng, L.; Shao, M.; Wang, W.; Huang, Y.; Wang, Y.; Zhu, Y.; Li, Y.; Hu, J.; Pan, B.; Cai, L.; Cheng, Y.; Ji, Y.; Zhang, F.; Rosenfeld, D.; Liss, P. S.; Duce, R. A.; Kolb, C. E.; Molina, M. J. Persistent sulfate formation from London Fog to Chinese haze. *Proc. Natl. Acad. Sci. U. S. A.* **2016**, *113*, 13630−13635.
(23) Guo, H.; Weber, R. J.; Nenes, A. High levels of ammonia do not raise fine particle pH sufficiently to yield nitrogen oxide-dominated sulfate production. *Sci. Rep.* **2017**, *7*, 12109.
(24) Wang, X.; Gemayel, R.; Hayeck, N.; Perrier, S.; Charbonnel, N.; Xu, C.; Chen, H.; Zhu, C.; Zhang, L.; Wang, L. Atmospheric photosensitization: a new pathway for sulfate formation. *Environ. Sci. Technol.* **2020**, *54*, 3114−3120.
(25) Jickells, T. D.; An, Z. S.; Andersen, K. K.; Baker, A. R.; Bergametti, G.; Brooks, N.; Cao, J. J.; Boyd, P. W.; Duce, R. A.; Hunter, K. A.; Kawahata, H.; Kubilay, N.; laRoche, J.; Liss, P. S.; Mahowald, N.; Prospero, J. M.; Ridgwell, A. J.; Tegen, I.; Torres, R. Global iron connections between desert dust, ocean biogeochemistry, and climate. *Science* **2005**, *308*, 67−71.
(26) Barkley, A. E.; Prospero, J. M.; Mahowald, N.; Hamilton, D. S.; Popendorf, K. J.; Oehlert, A. M.; Pourmand, A.; Gatineau, A.; Panechou-Pulcherie, K.; Blackwelder, P.; Gaston, C. J. African biomass burning is a substantial source of phosphorus deposition to the Amazon, Tropical Atlantic Ocean, and Southern Ocean. *Proc. Natl. Acad. Sci. U. S. A.* **2019**, *116*, 16216−16221.
(27) Fang, T.; Guo, H. Y.; Zeng, L. H.; Verma, V.; Nenes, A.; Weber, R. J. Highly Acidic Ambient Particles, Soluble Metals, and Oxidative Potential: A Link between Sulfate and Aerosol Toxicity. *Environ. Sci. Technol.* **2017**, *51*, 2611−2620.
(28) Buck, R. P.; Rondinini, S.; Covington, A. K.; Baucke, F. G. K.; Brett, C. M. A.; Camoes, M. F.; Milton, M. J. T.; Mussini, T.; Naumann, R.; Pratt, K. W.; Spitzer, P.; Wilson, G. S. Measurement of pH. Definition, standards, and procedures. *Pure Appl. Chem.* **2002**, *74*, 2169−2200.
(29) Zelenyuk, A.; Imre, D.; Cuadra-Rodriguez, L. A. Evaporation of water from particles in the aerodynamic lens inlet: An experimental study. *Anal. Chem.* **2006**, *78*, 6942−6947.
(30) Koutrakis, P.; Wolfson, J. M.; Slater, J. L.; Brauer, M.; Spengler, J. D.; Stevens, R. K.; Stone, C. L. Evaluation of an annular denuder/filter pack system to collect acidic aerosols and gases. *Environ. Sci. Technol.* **1988**, *22*, 1463−1468.
(31) Hennigan, C. J.; Izumi, J.; Sullivan, A. P.; Weber, R. J.; Nenes, A. A critical evaluation of proxy methods used to estimate the acidity of atmospheric particles. *Atmos. Chem. Phys.* **2015**, *15*, 2775−2790.
(32) Kanakidou, M.; Seinfeld, J. H.; Pandis, S. N.; Barnes, I.; Dentener, F. J.; Facchini, M. C.; Van Dingenen, R.; Ervens, B.; Nenes, A.; Nielsen, C. J.; Swietlicki, E.; Putaud, J. P.; Balkanski, Y.; Fuzzi, S.; Horth, J.; Moortgat, G. K.; Winterhalter, R.; Myhre, C. E. L.; Tsigaridis, K.; Vignati, E.; Stephanou, E. G.; Wilson, J. Organic aerosol and global climate modelling: a review. *Atmos. Chem. Phys.* **2005**, *5*, 1053−1123.
(33) Shiraiwa, M.; Li, Y.; Tsimpidi, A. P.; Karydis, V. A.; Berkemeier, T.; Pandis, S. N.; Lelieveld, J.; Koop, T.; Pöschl, U. Global distribution of particle phase state in atmospheric secondary organic aerosols. *Nat. Commun.* **2017**, *8*, 15002.
(34) Vander Wall, A. C.; Perraud, V.; Wingen, L. M.; Finlayson-Pitts, B. J. Evidence for a kinetically controlled burying mechanism for growth of high viscosity secondary organic aerosol. *Environ. Sci.: Processes Impacts* **2020**, *22*, 66−83.
(35) Silvern, R. F.; Jacob, D. J.; Kim, P. S.; Marais, E. A.; Turner, J. R.; Campuzano-Jost, P.; Jimenez, J. L. Inconsistency of ammonium-sulfate aerosol ratios with thermodynamic models in the eastern US: a possible role of organic aerosol. *Atmos. Chem. Phys.* **2017**, *17*, 5107.
(36) Zhang, Y.; Chen, Y.; Lei, Z.; Olson, N.; Riva, M.; Koss, A. R.; Zhang, Z.; Gold, A.; Jayne, J. T.; Worsnop, D. R.; Onasch, T. B.; Kroll, J. H.; Turpin, B. J.; Ault, A. P.; Surratt, J. D. Joint Impacts of Acidity and Viscosity on the Formation of Secondary Organic Aerosol from Isoprene Epoxydiols (IEPOX) in Phase Separated Particles. *ACS Earth Space Chem.* **2019**, *3*, 2646−2658.
(37) Schmedding, R.; Ma, M.; Zhang, Y.; Farrell, S.; Pye, H. O. T.; Chen, Y.; Wang, C.-t.; Rasool, Q. Z.; Budisulistiorini, S. H.; Ault, A. P.; Surratt, J. D.; Vizuete, W. α-Pinene-Derived organic coatings on acidic sulfate aerosol impacts secondary organic aerosol formation from isoprene in a box model. *Atmos. Environ.* **2019**, *213*, 456−462.
(38) Wexler, A. S.; Clegg, S. L. Atmospheric aerosol models for systems including the ions H^+, $NH4^+$, Na^+, SO_4^{2-}, NO_3^-, Cl^-, Br^-, and H_2O. *J. Geophys. Res.* **2002**, *107*, ACH 14-1−ACH 14-14.
(39) Clegg, S. L.; Seinfeld, J. H.; Brimblecombe, P. Thermodynamic modelling of aqueous aerosols containing electrolytes and dissolved organic compounds. *J. Aerosol Sci.* **2001**, *32*, 713−738.
(40) Nenes, A.; Pandis, S. N.; Pilinis, C. ISORROPIA: A new thermodynamic equilibrium model for multiphase multicomponent inorganic aerosols. *Aquat. Geochem.* **1998**, *4*, 123−152.
(41) Zuend, A.; Marcolli, C.; Booth, A. M.; Lienhard, D. M.; Soonsin, V.; Krieger, U. K.; Topping, D. O.; McFiggans, G.; Peter, T.; Seinfeld, J. H. New and extended parameterization of the thermodynamic model AIOMFAC: calculation of activity coefficients for organic-inorganic mixtures containing carboxyl, hydroxyl, carbonyl, ether, ester, alkenyl, alkyl, and aromatic functional groups. *Atmos. Chem. Phys.* **2011**, *11*, 9155−9206.
(42) Zuend, A.; Marcolli, C.; Luo, B. P.; Peter, T. A thermodynamic model of mixed organic-inorganic aerosols to predict activity coefficients. *Atmos. Chem. Phys.* **2008**, *8*, 4559−4593.
(43) Zaveri, R. A.; Easter, R. C.; Fast, J. D.; Peters, L. K. Model for Simulating Aerosol Interactions and Chemistry (MOSAIC). *J. Geophys. Res.* **2008**, DOI: 10.1029/2007JD008782.
(44) Pye, H. O. T.; Nenes, A.; Alexander, B.; Ault, A. P.; Barth, M. C.; Clegg, S. L.; Collett, J. L., Jr; Fahey, K. M.; Hennigan, C. J.; Herrmann, H.; Kanakidou, M.; Kelly, J. T.; Ku, I. T.; McNeill, V. F.; Riemer, N.; Schaefer, T.; Shi, G.; Tilgner, A.; Walker, J. T.; Wang, T.; Weber, R.; Xing, J.; Zaveri, R. A.; Zuend, A. The acidity of atmospheric particles and clouds. *Atmos. Chem. Phys.* **2020**, *20*, 4809−4888.
(45) Finlayson-Pitts, B. J.; Pitts, J. N. *Chemistry of the Upper and Lower Atmosphere*; Academic Press: San Diego, CA, 2000; DOI: 10.1016/B978-0-12-257060-5.X5000-X.

https://dx.doi.org/10.1021/acs.accounts.0c00303
Acc. Chem. Res. XXXX, XXX, XXX−XXX

(46) Weber, R. J.; Guo, H. Y.; Russell, A. G.; Nenes, A. High aerosol acidity despite declining atmospheric sulfate concentrations over the past 15 years. *Nat. Geosci.* **2016**, *9*, 282−285.
(47) Riemer, N.; Ault, A. P.; West, M.; Craig, R. L.; Curtis, J. H. Aerosol Mixing State: Measurements, Modeling, and Impacts. *Rev. Geophys.* **2019**, *57*, 187−249.
(48) Prather, K. A.; Hatch, C. D.; Grassian, V. H. Analysis of Atmospheric Aerosols. *Annu. Rev. Anal. Chem.* **2008**, *1*, 485−514.
(49) Craig, R. L.; Ault, A. P. Aerosol Acidity: Direct Measurement from a Spectroscopic Method. In *Multiphase Environmental Chemistry in the Atmosphere*; ACS Symposium Series 1299; American Chemical Society: 2018; Vol. *1299*, pp 171−191, DOI: 10.1021/bk-2018-1299.ch009.
(50) Bondy, A. L.; Wang, B.; Laskin, A.; Craig, R. L.; Nhliziyo, M. V.; Bertman, S. B.; Pratt, K. A.; Shepson, P. B.; Ault, A. P. Inland Sea Spray Aerosol Transport and Incomplete Chloride Depletion: Varying Degrees of Reactive Processing Observed during SOAS. *Environ. Sci. Technol.* **2017**, *51*, 9533−9542.
(51) Keene, W. C.; Pszenny, A. A. P.; Maben, J. R.; Sander, R. Variation of marine aerosol acidity with particle size. *Geophys. Res. Lett.* **2002**, *29*, 5-1−5-4.
(52) Gard, E. E.; Kleeman, M. J.; Gross, D. S.; Hughes, L. S.; Allen, J. O.; Morrical, B. D.; Fergenson, D. P.; Dienes, T.; Galli, M. E.; Johnson, R. J.; Cass, G. R.; Prather, K. A. Direct observation of heterogeneous chemistry in the atmosphere. *Science* **1998**, *279*, 1184−1187.
(53) Rindelaub, J. D.; Craig, R. L.; Nandy, L.; Bondy, A. L.; Dutcher, C. S.; Shepson, P. B.; Ault, A. P. Direct Measurement of pH in Individual Particles via Raman Microspectroscopy and Variation in Acidity with Relative Humidity. *J. Phys. Chem. A* **2016**, *120*, 911−917.
(54) Olson, N. E.; Lei, Z.; Craig, R. L.; Zhang, Y.; Chen, Y.; Lambe, A. T.; Zhang, Z.; Gold, A.; Surratt, J. D.; Ault, A. P. Reactive Uptake of Isoprene Epoxydiols Increases the Viscosity of the Core of Phase-Separated Aerosol Particles. *ACS Earth Space Chem.* **2019**, *3*, 1402−1414.
(55) Craig, R. L.; Bondy, A. L.; Ault, A. P. Surface Enhanced Raman Spectroscopy Enables Observations of Previously Undetectable Secondary Organic Aerosol Components at the Individual Particle Level. *Anal. Chem.* **2015**, *87*, 7510−7514.
(56) Creamean, J. M.; Axson, J. L.; Bondy, A. L.; Craig, R. L.; May, N. W.; Shen, H.; Weber, M. H.; Pratt, K. A.; Ault, A. P. Changes in precipitating snow chemistry with location and elevation in the California Sierra Nevada. *J. Geophys. Res.: Atmos.* **2016**, *121*, 7296−7309.
(57) Tirella, P. N.; Craig, R. L.; Tubbs, D. B.; Olson, N. E.; Lei, Z.; Ault, A. P. Extending surface enhanced Raman spectroscopy (SERS) of atmospheric aerosol particles to the accumulation mode (150−800 nm). *Environ. Sci.: Processes Impacts* **2018**, *20*, 1570−1580.
(58) Dazzi, A.; Prater, C. B. AFM-IR: Technology and applications in nanoscale infrared spectroscopy and chemical imaging. *Chem. Rev.* **2017**, *117*, 5146−5173.
(59) Bondy, A. L.; Kirpes, R. M.; Merzel, R. L.; Pratt, K. A.; Banaszak Holl, M. M.; Ault, A. P. Atomic Force Microscopy-Infrared Spectroscopy of Individual Atmospheric Aerosol Particles: Subdiffraction Limit Vibrational Spectroscopy and Morphological Analysis. *Anal. Chem.* **2017**, *89*, 8594−8598.
(60) Kirpes, R. M.; Rodriguez, B.; Kim, S.; China, S.; Laskin, A.; Park, K.; Jung, J.; Ault, A. P.; Pratt, K. A. Emerging investigator series: influence of marine emissions and atmospheric processing on individual particle composition of summertime Arctic aerosol over the Bering Strait and Chukchi Sea. *Environ. Sci.: Processes Impacts* **2020**, *22*, 1201−1213.
(61) Or, V. W.; Estillore, A.; Grassian, V.; Tivanski, A. V. Lab on a Tip: Atomic Force Microscopy-Photothermal Infrared Spectroscopy of Atmospherically Relevant Organic/Inorganic Aerosol Particles in the Nanometer to Micrometer Size Range. *Analyst* **2018**, *143*, 2765−2774.
(62) Or, V. W.; Alves, M. R.; Wade, M.; Schwab, S.; Corsi, R. L.; Grassian, V. H. Crystal Clear? Microspectroscopic Imaging and Physicochemical Characterization of Indoor Depositions on Window Glass. *Environ. Sci. Technol. Lett.* **2018**, *5*, 514−519.
(63) Olson, N. E.; Xiao, Y.; Lei, Z.; Ault, A. P. Simultaneous Optical Photothermal Infrared (O-PTIR) and Raman Spectroscopy of Submicrometer Atmospheric Particles. *Anal. Chem.* **2020**, *92*, 9932−9939.
(64) Lide, D. R., Ed.; *CRC Handbook of Chemistry and Physics*; 89th ed.; CRC Press/Taylor and Francis: Boca Raton, FL, 2009; DOI: 10.1080/08893110902764125.
(65) Dutcher, C. S.; Ge, X.; Wexler, A. S.; Clegg, S. L. An Isotherm-Based Thermodynamic Model of Multicomponent Aqueous Solutions, Applicable Over the Entire Concentration Range. *J. Phys. Chem. A* **2013**, *117*, 3198−3213.
(66) Guo, H.; Xu, L.; Bougiatioti, A.; Cerully, K. M.; Capps, S. L.; Hite, J. R., Jr.; Carlton, A. G.; Lee, S. H.; Bergin, M. H.; Ng, N. L.; Nenes, A.; Weber, R. J. Fine-particle water and pH in the southeastern United States. *Atmos. Chem. Phys.* **2015**, *15*, 5211−5228.
(67) Pope, C. A.; Dockery, D. W. Health effects of fine particulate air pollution: Lines that connect. *J. Air Waste Manage. Assoc.* **2006**, *56*, 709−742.
(68) Coddens, E. M.; Angle, K. J.; Grassian, V. H. Titration of Aerosol pH through Droplet Coalescence. *J. Phys. Chem. Lett.* **2019**, *10*, 4476−4483.
(69) Boyer, H. C.; Gorkowski, K.; Sullivan, R. C. In situ pH measurements of individual levitated microdroplets using aerosol optical tweezers. *Anal. Chem.* **2020**, *92*, 1089−1096.
(70) Li, G.; Su, H.; Ma, N.; Zheng, G.; Kuhn, U.; Li, M.; Klimach, T.; Pöschl, U.; Cheng, Y. Multifactor colorimetric analysis on pH-indicator papers: an optimized approach for direct determination of ambient aerosol pH. *Atmos. Meas. Technol. Discuss.* **2019**, in review.
(71) Slade, J. H.; Ault, A. P.; Bui, A. T.; Ditto, J. C.; Lei, Z.; Bondy, A. L.; Olson, N. E.; Cook, R. D.; Desrochers, S. J.; Harvey, R. M.; Erickson, M. H.; Wallace, H. W.; Alvarez, S. L.; Flynn, J. H.; Boor, B. E.; Petrucci, G. A.; Gentner, D. R.; Griffin, R. J.; Shepson, P. B. Bouncier Particles at Night: Biogenic Secondary Organic Aerosol Chemistry and Sulfate Drive Diel Variations in the Aerosol Phase in a Mixed Forest. *Environ. Sci. Technol.* **2019**, *53*, 4977−4987.
(72) Freedman, M. A. Phase separation in organic aerosol. *Chem. Soc. Rev.* **2017**, *46*, 7694−7705.
(73) Gervasi, N. R.; Topping, D. O.; Zuend, A. A predictive group-contribution model for the viscosity of aqueous organic aerosol. *Atmos. Chem. Phys.* **2020**, *20*, 2987−3008.
(74) Zhang, Y.; Chen, Y.; Lambe, A. T.; Olson, N. E.; Lei, Z.; Craig, R. L.; Zhang, Z.; Gold, A.; Onasch, T. B.; Jayne, J. T.; Worsnop, D. R.; Gaston, C. J.; Thornton, J. A.; Vizuete, W.; Ault, A. P.; Surratt, J. D. Effect of the Aerosol-Phase State on Secondary Organic Aerosol Formation from the Reactive Uptake of Isoprene-Derived Epoxydiols (IEPOX). *Environ. Sci. Technol. Lett.* **2018**, *5*, 167−174.
(75) Schmedding, R.; Ma, M.; Zhang, Y.; Farrell, S.; Pye, H. O. T.; Chen, Y.; Wang, C.-t.; Rasool, Q. Z.; Budisulistiorini, S. H.; Ault, A. P.; Surratt, J. D.; Vizuete, W. α-Pinene-Derived organic coatings on acidic sulfate aerosol impacts secondary organic aerosol formation from isoprene in a box model. *Atmos. Environ.* **2019**, *213*, 456−462.
(76) Riva, M.; Chen, Y.; Zhang, Y.; Lei, Z.; Olson, N. E.; Boyer, H. C.; Narayan, S.; Yee, L. D.; Green, H. S.; Cui, T.; Zhang, Z.; Baumann, K.; Fort, M.; Edgerton, E.; Budisulistiorini, S. H.; Rose, C. A.; Ribeiro, I. O.; e Oliveira, R. L.; dos Santos, E. O.; Machado, C. M. D.; Szopa, S.; Zhao, Y.; Alves, E. G.; de Sá, S. S.; Hu, W.; Knipping, E. M.; Shaw, S. L.; Duvoisin Junior, S.; de Souza, R. A. F.; Palm, B. B.; Jimenez, J.-L.; Glasius, M.; Goldstein, A. H.; Pye, H. O. T.; Gold, A.; Turpin, B. J.; Vizuete, W.; Martin, S. T.; Thornton, J. A.; Dutcher, C. S.; Ault, A. P.; Surratt, J. D. Increasing Isoprene Epoxydiol-to-Inorganic Sulfate Aerosol Ratio Results in Extensive Conversion of Inorganic Sulfate to Organosulfur Forms: Implications for Aerosol Physicochemical Properties. *Environ. Sci. Technol.* **2019**, *53*, 8682−8694.
(77) Jungwirth, P.; Tobias, D. J. Specific ion effects at the air/water interface. *Chem. Rev.* **2006**, *106*, 1259−1281.
(78) Crans, D. C.; Levinger, N. E. The Conundrum of pH in Water Nanodroplets: Sensing pH in Reverse Micelle Water Pools. *Acc. Chem. Res.* **2012**, *45*, 1637−1645.

https://dx.doi.org/10.1021/acs.accounts.0c00303
Acc. Chem. Res. XXXX, XXX, XXX−XXX

(79) Muñoz-Santiburcio, D.; Marx, D. Chemistry in nanoconfined water. *Chem. Sci.* **2017**, *8*, 3444−3452.
(80) Enami, S.; Stewart, L. A.; Hoffmann, M. R.; Colussi, A. J. Superacid Chemistry on Mildly Acidic Water. *J. Phys. Chem. Lett.* **2010**, *1*, 3488−3493.
(81) Lee, J. K.; Samanta, D.; Nam, H. G.; Zare, R. N. Micrometer-Sized Water Droplets Induce Spontaneous Reduction. *J. Am. Chem. Soc.* **2019**, *141*, 10585−10589.

https://dx.doi.org/10.1021/acs.accounts.0c00303
Acc. Chem. Res. XXXX, XXX, XXX−XXX